In vivo imaging of Lgr5-positive cell populations using confocal laser endomicroscopy during early colon tumorigenesis

Authors Jin Woo Choi[1,2,*], Jun Ki Kim[3,*], Myunghwan Choi[1], Yi Rang Kim[1], Seok Hyun Yun[1]

Institutions Institutions are listed at the end of article.

submitted
18. February 2014
accepted after revision
2. July 2014

Bibliography
DOI http://dx.doi.org/10.1055/s-0034-1377631
Published online: 12.9.2014
Endoscopy 2014; 46: 1110–1115
© Georg Thieme Verlag KG Stuttgart · New York
ISSN 0013-726X

Corresponding author
Seok Hyun Yun, MD
Wellman Center
Harvard Medical School
40 Blossom Street
Boston
Massachusetts 02114
United States
Fax: +1-617-6328449
syun@hms.harvard.edu

Background and study aims: A diagnostic molecular marker for pre-neoplastic lesions, particularly before polyposis, is still lacking. Lgr5 has been broadly accepted as a marker for intestinal cancer stem cells. The aim of this study was to investigate the monitoring of Lgr5$^+$ cells as a useful tool for the early diagnosis of premalignant lesions before polyp formation.

Methods: In vivo molecular imaging was performed to examine colon tumorigenesis in *Lgr5-EGFP* mice treated with azoxymethane and dextran sodium sulfate. eGFP$^+$ Lgr5$^+$ regions in the descending colon were longitudinally monitored using side-view confocal endomicroscopy. Based on the eGFP signal intensity on the luminal surface, polyps were classified into two groups – Lgr5-high and Lgr5-low. White light colonoscopy was used to monitor polyp formation.

Results: Approximately 75 % of the polyps originated from foci containing Lgr5-eGFP$^+$ cells, whereas 25 % of the polyps emerged from Lgr5$^-$ foci. Among eGFP$^+$ foci, Lgr5-high foci grew faster than Lgr5-low foci.

Conclusions: Polyps developed at Lgr5$^+$ regions. Luminal Lgr5 expression was correlated with the growth rate of early-stage adenomas. Lgr5 is a promising molecular marker for the early diagnosis of colon tumors.

Introduction

Colorectal cancer is preceded by a pre-invasive (adenoma) state that lasts for several years [1]. Early detection and resection of adenomas are important to prevent colon cancer. Current endoscopic procedures using conventional endoscopes have several drawbacks. Colon tumors that are expressed as flat or mildly elevated focal lesions are hard to detect [2]. Discriminating tumors from gross surrounding inflammatory lesions is difficult in cases with underlying inflammatory bowel disease, such as ulcerative colitis and Crohn's disease [3]. To overcome these problems, novel endoscopic techniques, including narrow-band imaging endoscopy [4,5], autofluorescence endoscopy [4,5], and confocal laser endomicroscopy (CLE) [6,7], have been introduced to improve clinical precision of cancer detection. Fluorescence imaging targeting specific molecular markers for pre-cancerous lesions can greatly improve early detection, but reliable biomarkers are currently lacking.

Stem-cell markers are promising candidates. Lgr5 is one of the most reliable intestinal stem-cell markers [8]. Lgr5$^+$ cells predominantly populate adenomas. Lgr5$^+$ cells were found within tumors in an *Apc*-knockout mouse model, and were shown to promote the growth of adenomas in the small intestine [9]. These results suggest that Lgr5 may define intestinal cancer stem cells as well as normal stem cells.

This report describes in vivo observation of Lgr5$^+$ cells in a mouse model of chemically induced, early tumorigenesis using the recently developed side-view CLE [10], which enabled cellular imaging of the murine gastrointestinal tract over a wide area.

Methods

Tumorigenesis

Lgr5-EGFP-IRES-creERT2 knock-in transgenic mice (*Lgr5-EGFP* mice) were purchased from Jackson Laboratories (strain: B6.129P2-*Lgr5tm1(cre/ERT2)Cle*/J). *Lgr5-EGFP* mice (8 weeks) were injected intraperitoneally with 10 mg/kg azoxymethane (AOM; Sigma-Aldrich Corp., St Louis, Missouri, USA). One week later, the mice were

* These authors contributed equally to this work.

Downloaded by: University of Ulsan. Copyrighted material.

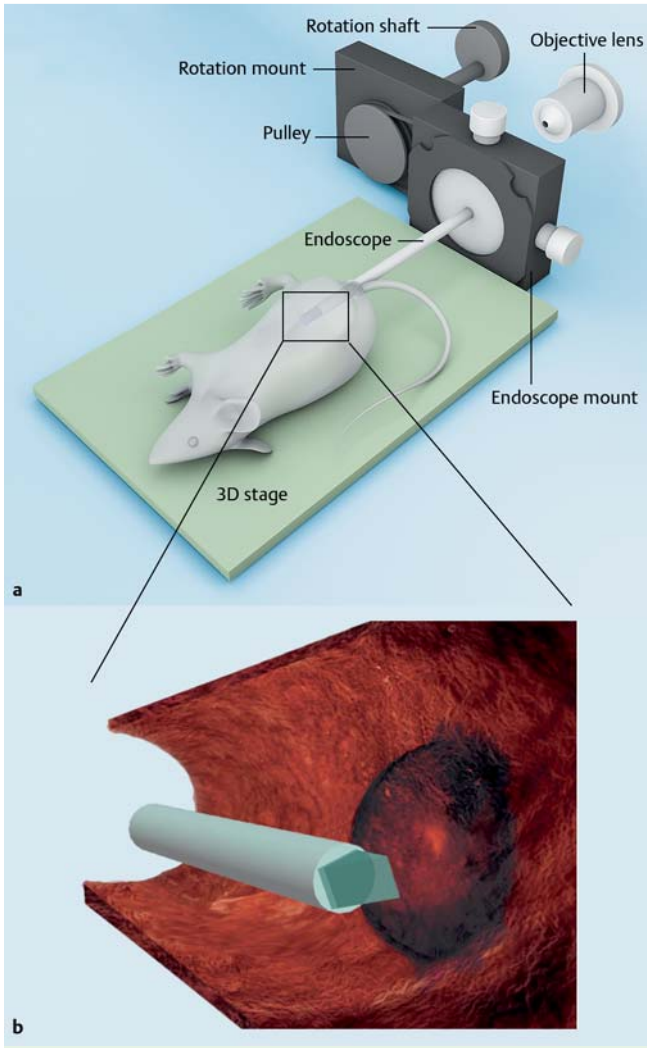

Fig. 1 In vivo colonoscopy. **a** Schematic of the experimental setup for endomicroscopy in the descending colon of an anesthetized mouse. **b** Illustration of side-view endomicroscopy.

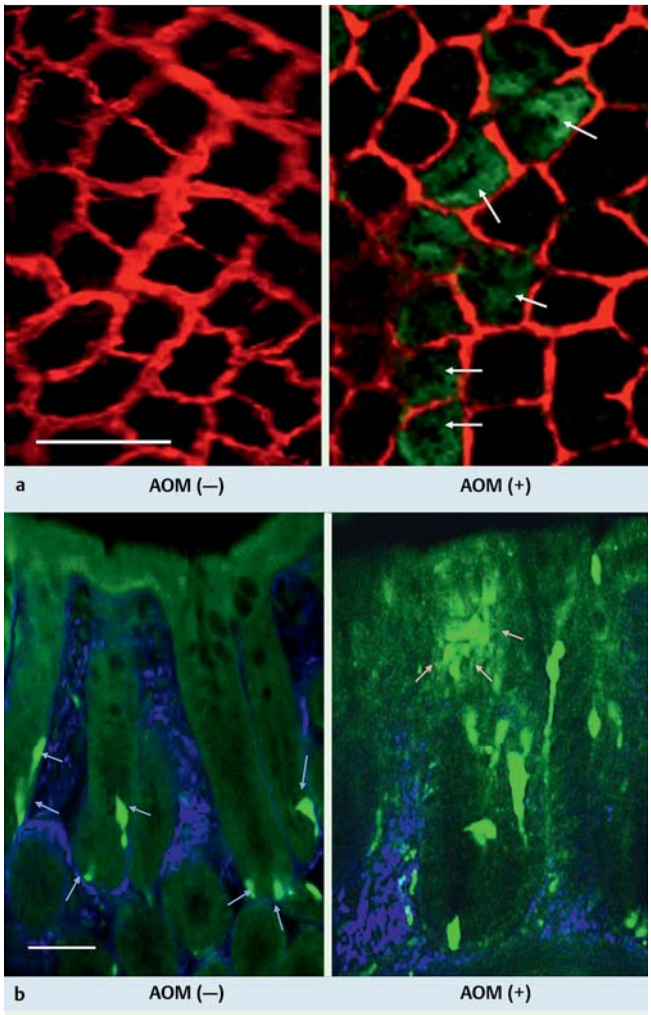

Fig. 2 Appearance of Lgr5-eGFP$^+$ sites. **a** Fluorescence images of a representative Lgr5-eGFP$^+$ region in the colonic luminal surface of an isolated murine colon. Green, eGFP signal; red, rhodamine–dextran in the vasculature. Scale bar, 100 µm. **b** Two-photon images of colonic tissues isolated from *Lgr5-EGFP* mice without (left) and 7 days after azoxymethane treatment (right) and cleared by benzyl alcohol/benzyl benzoate solution. Blue arrows indicate Lgr5-eGFP$^+$ cells in the bottom of the crypts, whereas pink arrows indicate Lgr5-eGFP$^+$ cells found near the apex of the crypts. Second harmonic generation signal (blue) from the collagen fibers delineate the crypt structure.

given 3% dextran sulfate sodium (DSS; MP Biochemicals, Santa Ana, California, USA) in drinking water for 5 days, followed by normal drinking water thereafter. The Institutional Animal Care and Use Committee of Massachusetts General Hospital approved the study.

Confocal endomicroscopy

A side-view optical probe (diameter 1.3 mm, length 5 cm) was inserted into the descending colon of mice that had been anesthetized by intraperitoneal administration of ketamine/xylazine (90 mg/9 mg per kg body weight) (**Fig. 1**). eGFP was visualized by 491 nm excitation and 502 – 537 nm fluorescence detection. For vasculature imaging, rhodamine–dextran conjugates (5 µg/µL, 2 000 000 MW; Invitrogen, Carlsbad, California, USA) were injected intravenously and imaged by 532 nm excitation and 562 – 596 nm detection. The coordinates (angle, distance from the anus) of each tumor were recorded to help identify the same foci in the subsequent imaging session.

White-light colonoscopy

A white-light telescopic endoscope (outer diameter 1.9 mm, ColoView; Karl Stortz GmbH, Tuttlingen, Germany) using a xenon lamp (XENON nova 175, Karl Stortz) was used to monitor polyps at the coordinates recorded during confocal imaging. The tumor size was estimated from 3-chip video images (width × height × 2), where the distance-dependent magnification was calibrated by imaging a ruler at the same distance as the tumor.

Cleared colon tissue imaging

Dissected colon tissues were cleared by using benzyl alcohol/benzyl benzoate solution (BABB) to increase the transparency for three-dimensional imaging of the crypt [11].

Downloaded by: University of Ulsan. Copyrighted material.

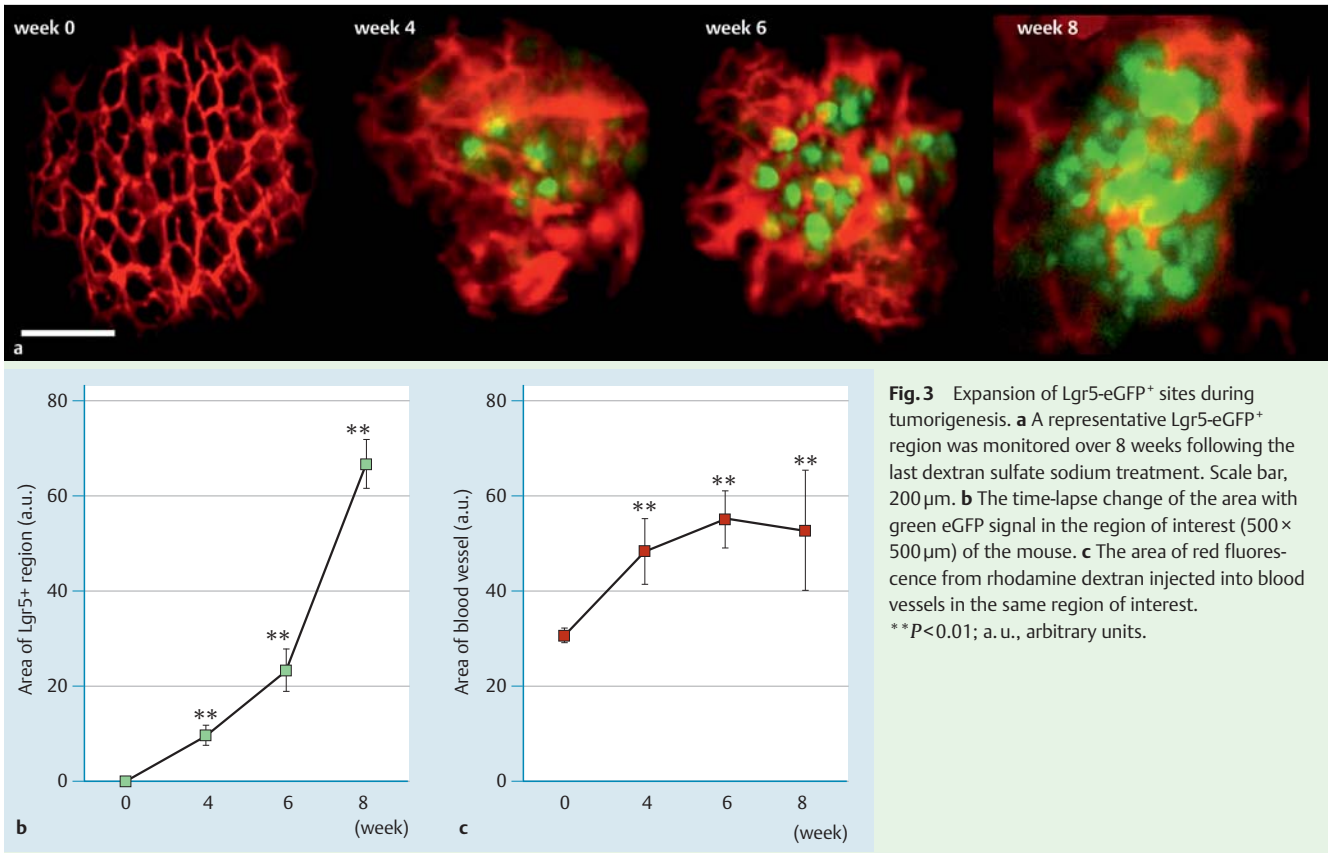

Fig. 3 Expansion of Lgr5-eGFP$^+$ sites during tumorigenesis. **a** A representative Lgr5-eGFP$^+$ region was monitored over 8 weeks following the last dextran sulfate sodium treatment. Scale bar, 200 µm. **b** The time-lapse change of the area with green eGFP signal in the region of interest (500 × 500 µm) of the mouse. **c** The area of red fluorescence from rhodamine dextran injected into blood vessels in the same region of interest. $^{**}P<0.01$; a.u., arbitrary units.

Results

Migration of Lgr5$^+$ cells to the colonic luminal surface after AOM treatment

Colon tumorigenesis was induced by a single injection of AOM or administration of AOM–DSS in *Lgr5-EGFP* mice. eGFP expression was then examined in the isolated colon segments using fluorescence microscopy. Under normal conditions, eGFP$^+$ regions were confined to the crypt bottom and were not observed on the luminal colon surfaces in *Lgr5-EGFP* mice (**Fig. 2a**). eGFP$^+$ foci emerged on the luminal surface 3 days after AOM treatment and were apparently confined to hexagonal vascular formations (**Fig. 2a**). To verify how the eGFP signal moved to the luminal surfaces, the Lgr5$^+$ cells along the luminal transverse sections were imaged. Under normal conditions, Lgr5$^+$ cells were confined to deep within the crypts (**Fig. 2b**). Upon AOM treatment, Lgr5$^+$ cells formed clusters of 5 – 10 cells at luminal foci (**Fig. 2b**). Taken together, Lgr5$^+$ cells migrated to the luminal surfaces during AOM-induced tumorigenesis.

Imaging Lgr5$^+$ foci and the associated vasculature in vivo

A single AOM injection can induce microadenoma development and accompanying angiogenesis [12]. In vivo CLE revealed the progressive growth of Lgr5$^+$ foci and angiogenic vessels on the luminal colonic surfaces over time (**Fig. 3a**). The area of the eGFP$^+$ region increased exponentially over time (**Fig. 3b**). Vasculature changed from regular hexagonal lattices to irregularly formed networks over time after AOM treatment. Neovascular patterns together with high Lgr5$^+$ cell populations were readily observed 4 weeks after AOM treatment (**Fig. 3c**).

Emergence of polyps at Lgr5$^+$ foci

To induce polyposis, AOM treatment was followed by 3 % DSS administration at 1-week intervals. At 4 weeks after the AOM–DSS treatment, a total of 19 eGFP$^+$ regions were observed in seven mice by in vivo CLE and white-light colonoscopy (**Fig. 4a**). Only one small polyp was observed at week 4, but at week 10, 13 polyps emerged from the 19 eGFP$^+$ sites marked at week 4 (**Fig. 4b**). Five additional macroadenomas were found in these mice, but these polyps had emerged from eGFP-negative sites at weeks 8 – 10 (**Fig. 4c**). eGFP$^+$ regions were typically detected 2 – 4 weeks before the appearance of macroscopic polyps could be observed by white-light colonoscopy. This result indicates the potential of Lgr5 as an early diagnostic marker before polypsis.

Determination of tumor growth rate by Lgr5 expression level

Among the 18 tumors observed at week 10, 13 tumors had shown eGFP signals on the luminal surfaces at week 4. These were further classified into two groups – Lgr5-high (n = 7) and Lgr5-low (n = 6), based retrospectively on their average eGFP fluorescence intensity at week 4 (see Supplementary **Fig. e5**, available online). The difference in Lgr5 expression was confirmed by immunostaining and BABB-clearing imaging with isolated polyps (see Supplementary **Fig. e6**, available online). From the longitudinal data obtained using white-light colonoscopy, it was found that tumors derived from Lgr5-high foci grew faster and larger than those originating from Lgr5-low foci (**Fig. 7a, b**). Histopathology at week 12 indicated a significant size difference between two representative tumors (**Fig. 7c**).

Downloaded by: University of Ulsan. Copyrighted material.

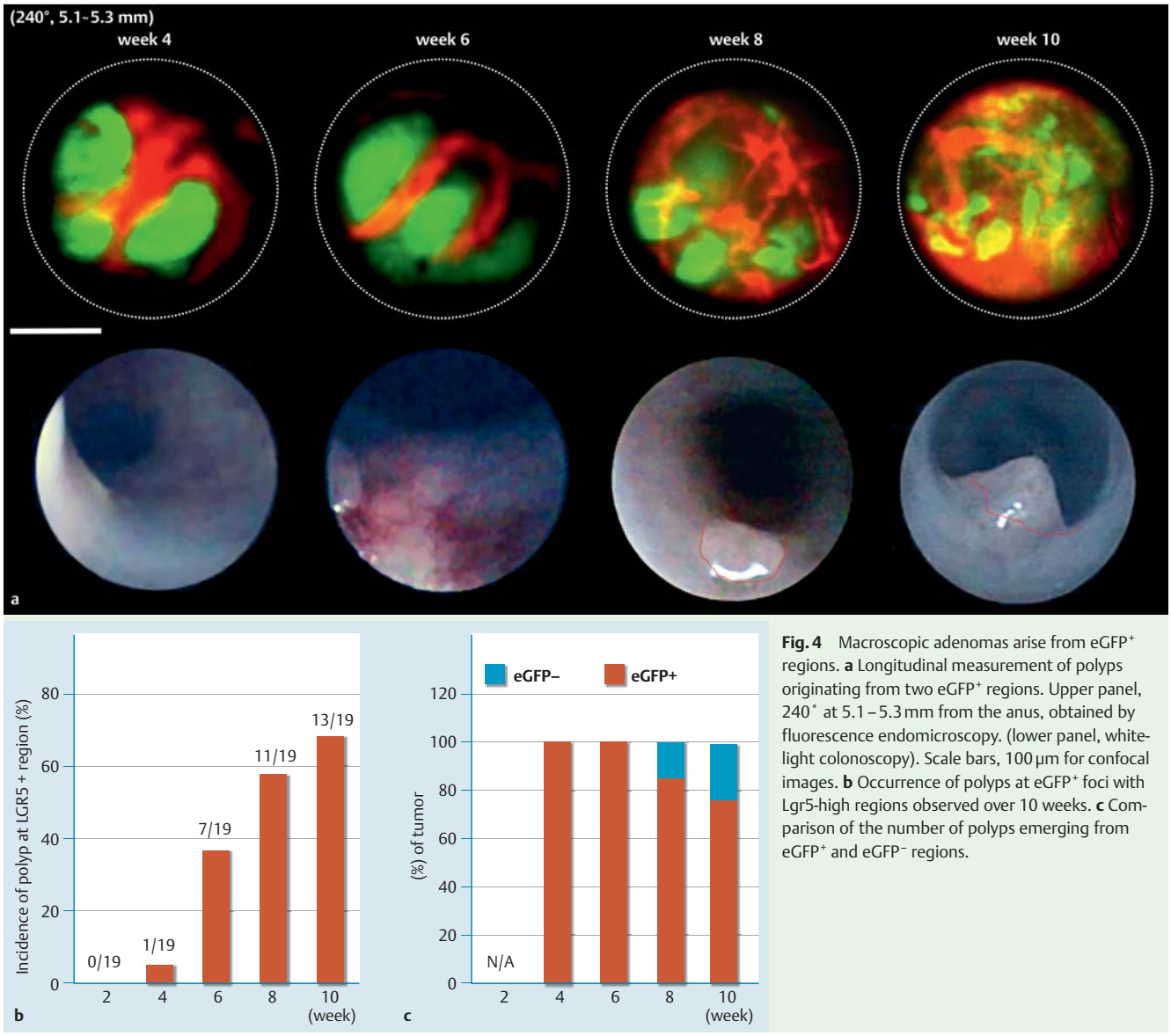

Fig. 4 Macroscopic adenomas arise from eGFP$^+$ regions. **a** Longitudinal measurement of polyps originating from two eGFP$^+$ regions. Upper panel, 240° at 5.1 – 5.3 mm from the anus, obtained by fluorescence endomicroscopy. (lower panel, white-light colonoscopy). Scale bars, 100 µm for confocal images. **b** Occurrence of polyps at eGFP$^+$ foci with Lgr5-high regions observed over 10 weeks. **c** Comparison of the number of polyps emerging from eGFP$^+$ and eGFP$^-$ regions.

Discussion

Lgr5 is the most reliable marker for intestinal cancer stem cells as well as normal stem cells. In a previous study, Lgr5 was reported to contribute to noninflammatory cancers [9]. In the current work, AOM and DSS were used to mimic inflammation-associated tumorigenesis [13]. In early stages of tumorigenesis before polyposis, Lgr5$^+$ cells that emerged on the colonic luminal surfaces could be readily detectable with the help of appropriate fluorescent probes by CLE. According to the current data, Lgr5 expression within tumors was correlated with the growth rate of early-stage adenomas in the inflammatory murine models. Thus, Lgr5$^+$ cells may be used as an early diagnostic marker in both noninflammatory and inflammation-associated colon tumors.

Through combination of Lgr5 and CLE, this study demonstrated the potential to predict the growth of colonic tumorigenesis foci much earlier than they would be visible by conventional white-light colonoscopy. Although eGFP-transgenic mice were used to monitor the role of Lgr5$^+$ cells in this research, fluorescence-labeled antibody against Lgr5 can be clinically used to mark Lgr5$^+$ cells in the near future. As a result, these likely tumor sites can be removed easily in their initial stages without using high-risk endoscopic procedures such as endoscopic mucosal resection or endoscopic submucosal dissection. Furthermore, CLE for visualization of Lgr5$^+$ cells may become a predictive tool for prognosis after surgery. As disease relapse can be anticipated by measuring Lgr5 expression levels, tumor regrowth after surgery may be monitored by observing the extent of Lgr5$^+$ sites on luminal surfaces. Furthermore, Lgr5$^+$ cells may be appropriate targets for preventive therapies.

In summary, the CLE technique enabled detection of Lgr5$^+$ cells and may improve colon cancer prevention and advance therapeutic interventions.

Downloaded by: University of Ulsan. Copyrighted material.

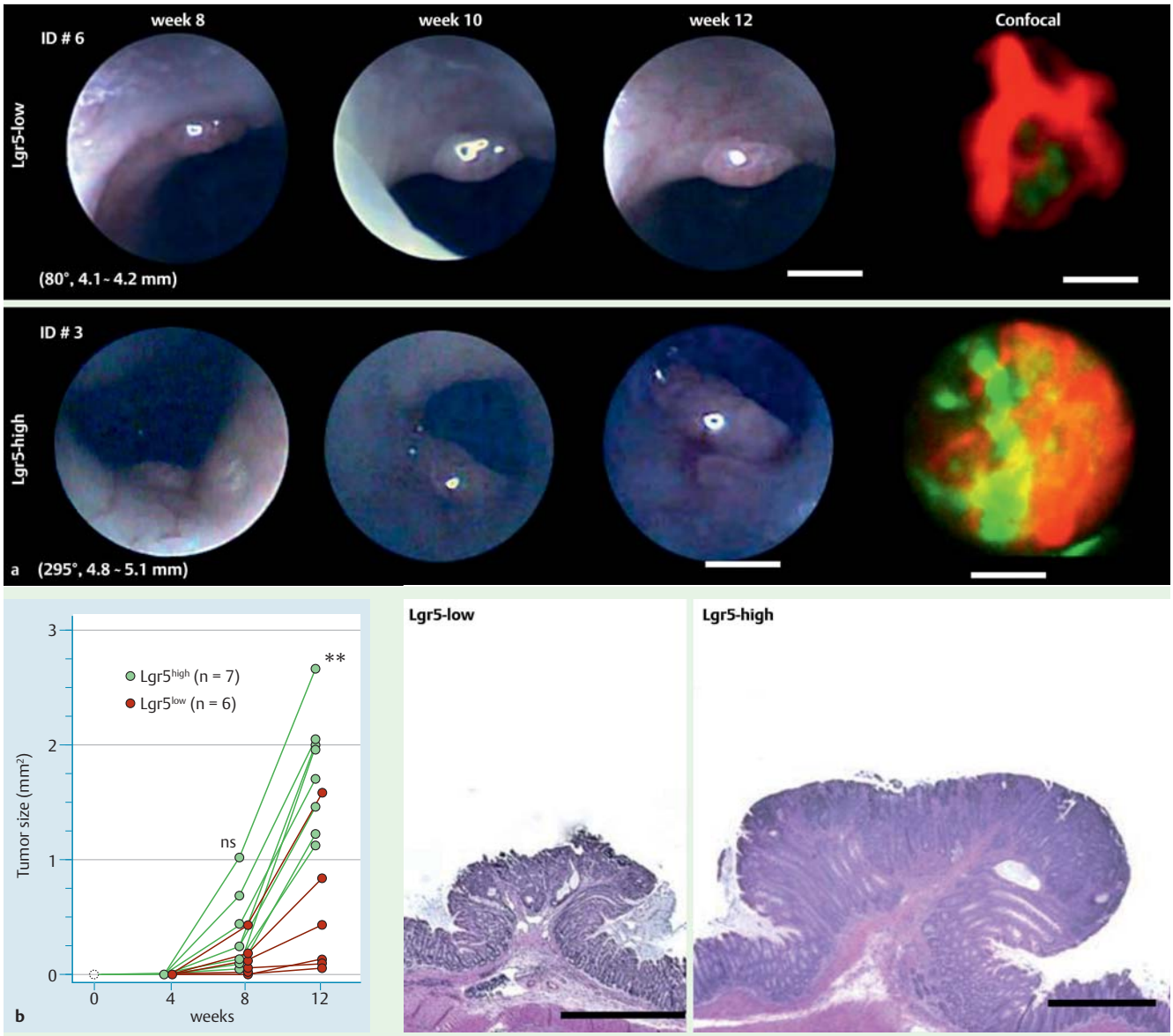

Fig. 7 Lgr5-high tumors grew faster than Lgr5-low tumors. **a** Longitudinal imaging of Lgr5-high and Lgr5-low polyps 8 – 12 weeks after AOM–DSS treatment. Scale bars, 100 µm for confocal images. **b** Tumor volumes measured over time for Lgr5-high (green, n = 7) and Lgr5-low (pink, n = 6) tumors. **c** Representative Lgr5-low and Lgr5-high tumors at week 12. Scale bar, 1 mm. $^{**}P<0.01$; n. s., not significant.

Downloaded by: University of Ulsan. Copyrighted material.

Competing interests: None

Institutions
[1] Wellman Center for Photomedicine, Massachusetts General Hospital, Harvard Medical School, Boston, Massachusetts, USA
[2] Department of Pharmacology and Institute of Dental Research, School of Dentistry, Wonkwang University, Iksan, Chonbuk, Korea
[3] Biomedical Engineering R&D Center, Asan Institute for Life Sciences, Asan Medical Center and University of Ulsan College of Medicine, Seoul, Korea

Acknowledgments

This work was supported through grants from the National Institutes of Health (U54CA143837, P41EB015903) and the National Research Foundation of Korea (WCU R31-2008-000-10071-0, NRF-2011-357-C00141, and 2008-0062484).

References

1 *Hill MJ*, *Morson BC*, *Bussey HJ*. Aetiology of adenoma – carcinoma sequence in large bowel. Lancet 1978; 1: 245 – 247
2 *Kim CY*, *Fleischer DE*. Colonic chromoscopy. A new perspective on polyps and flat adenomas. Gastrointest Endosc Clin North Am 1997; 7: 423 – 437
3 *Eaden JA*, *Mayberry JF*. British Society for Gastroenterology; Association of Coloproctology for Great Britain and Ireland. Guidelines for screening and surveillance of asymptomatic colorectal cancer in patients with inflammatory bowel disease. Gut 2002; 51: V10 – 12
4 *Machida H*, *Sano Y*, *Hamamoto Y* et al. Narrow-band imaging in the diagnosis of colorectal mucosal lesions: a pilot study. Endoscopy 2004; 36: 1094 – 1098
5 *Ragunath K*. Autofluorescence endoscopy – not much gain after all? Endoscopy 2007; 39: 1021 – 1022
6 *Hurlstone DP*, *Baraza W*, *Brown S* et al. In vivo real-time confocal laser scanning endomicroscopic colonoscopy for the detection and characterization of colorectal neoplasia. Br J Surg 2008; 95: 636 – 645
7 *Sanduleanu S*, *Driessen A*, *Gomez-Garcia E* et al. In vivo diagnosis and classification of colorectal neoplasia by chromoendoscopy-guided confocal laser endomicroscopy. Clin Gastroenterol Hepatol 2010; 8: 371 – 378
8 *Barker N*, *van Es JH*, *Kuipers J* et al. Identification of stem cells in small intestine and colon by marker gene Lgr5. Nature 2007; 449: 1003 – 1007
9 *Barker N*, *Ridgway RA*, *van Es JH* et al. Crypt stem cells as the cells-of-origin of intestinal cancer. Nature 2009; 457: 608 – 611
10 *Kim P*, *Chung E*, *Yamashita H* et al. In vivo wide-area cellular imaging by side-view endomicroscopy. Nat Methods 2010; 7: 303 – 305
11 *Parra SG*, *Chia TH*, *Zinter JP* et al. Multiphoton microscopy of cleared mouse organs. J Biomed Optics 2010; 15: 036017
12 *Bird RP*. Observation and quantification of aberrant crypts in the murine colon treated with a colon carcinogen: preliminary findings. Cancer letters 1987; 37: 147 – 151
13 *Tanaka T*, *Kohno H*, *Suzuki R* et al. A novel inflammation-related mouse colon carcinogenesis model induced by azoxymethane and dextran sodium sulfate. Cancer Sci 2003; 94: 965 – 973

Figures e5 and e6

online content viewable at: www.thieme-connect.de

Downloaded by: University of Ulsan. Copyrighted material.

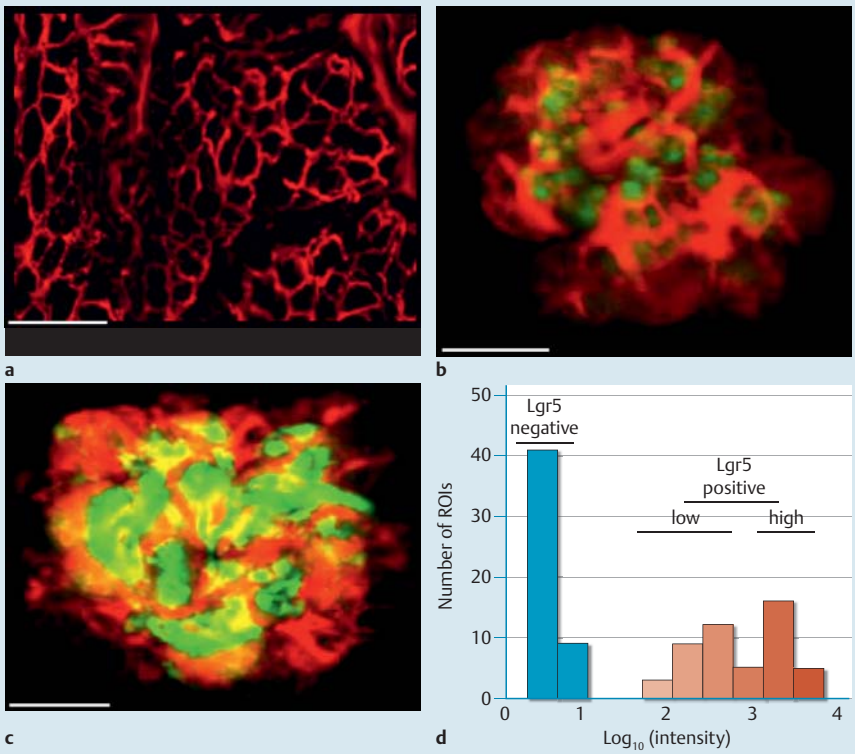

Fig. e5 Tumor categorization into Lgr5-low or Lgr5-high classes. Three representative regions with distinctly different densities of Lgr5-eGFP$^+$ cells (green). **a** No signal in normal vascular areas. Low (**b**) or high (**c**) eGFP expression accompanying irregular vascularture (red). Scale bars, 500 µm. **d** Histogram of eGFP fluorescence intensity analyzed with Image J 2.0. Log scale 3 was determined as the criterion to divide between "Lgr5-high" and "Lgr5-low" regions. ROI, region of interest.

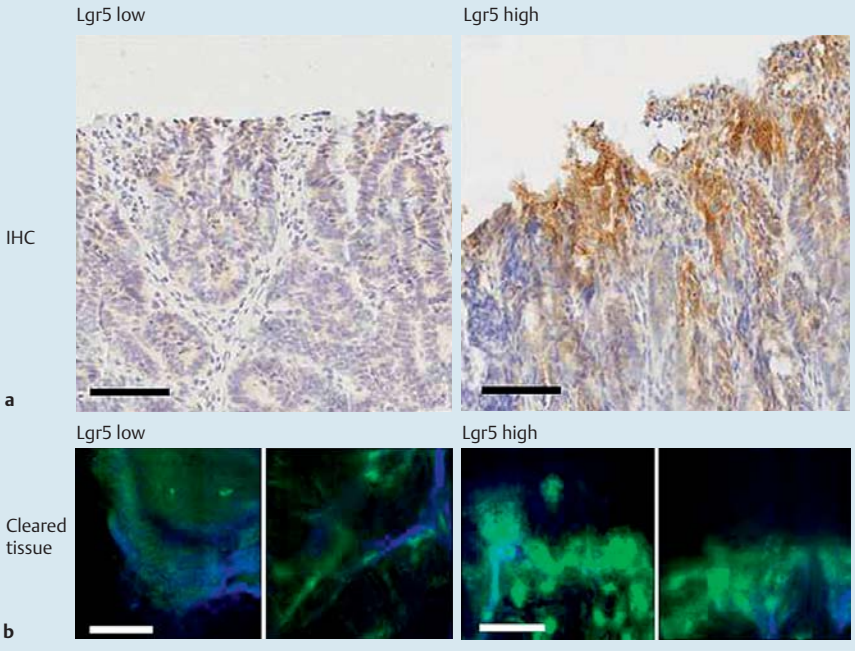

Fig. e6 Immunohistochemistry (IHC) of Lgr5-low and Lgr5-high tumors. **a** Colon tissues were fixed in 10 % formalin for 24 hours, dehydrated, and embedded in paraffin. After antigen retrieval, the slides were blocked with 4 % bovine serum albumin for 30 minutes and washed with phosphate buffered saline containing 0.1 % Tween 20. Polyclonal antibodies against Lgr5 (ab 75732) were added to the slides and incubated for 90 minutes. Scale bars, 200 µm. **b** Two-photon images of tumor tissues cleared by benzyl alcohol/benzyl benzoate solution, as described in the text. Scale bars, 100 µm.